Received 3 July 2020; revised 5 August 2020; accepted 16 September 2020. Date of publication 21 September 2020; date of current version 15 October 2020.
The review of this article was arranged by Editor P. Pavan.

Digital Object Identifier 10.1109/JEDS.2020.3025554

An Improved Self-Powered H-Bridge Circuit for Voltage Rectification of Piezoelectric Energy Harvesting System

MAHESH EDLA [1], YEE YAN LIM [1], MIKIO DEGUCHI [2], RICARDO VASQUEZ PADILLA [1], AND IMAN IZADGOSHASB [1]

1 School of Environmental Science and Engineering, Southern Cross University, Lismore, NSW 2480, Australia
2 Department of Environmental Materials Engineering, National Institute of Technology, Niihama College, Ehime 792-8580, Japan

CORRESPONDING AUTHOR: M. EDLA (e-mail: m.edla.10@student.scu.edu.au)

The work of Mahesh Edla was supported by Southern Cross University.

ABSTRACT In recent years, piezoelectric materials have been widely investigated for harvesting energy from ambient vibrations. A vibrating piezoelectric device (PD) generates alternating current (AC), which needs to be converted into direct current (DC) for powering electronic devices or for storage. A traditional full-wave bridge rectifier (FBR) interface circuit serves this purpose, but it suffers from high power loss due to the presence of high forward voltage across the diodes. In this article, an improved H-Bridge rectifier circuit is proposed as the AC-DC rectifier circuit to reduce power loss for high frequency and low amplitude application. The performance of the proposed rectifier circuit was experimentally studied, analysed and discussed. Two different testing scenarios for high frequency, namely, varying input power with fixed excitation frequency and varying excitation frequency with fixed input voltage were considered. Applicability of the circuit at low frequency range was also investigated. The outcome shows that the proposed circuit notably increases the voltage and the power produced from the PD when compared to traditional FBR circuits.

INDEX TERMS Piezoelectric energy harvesting, rectifier circuits, self-powered AC-DC circuit, H-bridge, MOSFET.

I. INTRODUCTION

High energy demand and consumption are some of the most critical challenges faced by modern society. Thus, scientists and researchers are persistently searching for renewable energy sources to reduce the reliance on unsustainable sources of energy. A wide range of energy sources are readily available in the environment, in the form of thermal [1], solar [2], wind [3] and mechanical energy [4]. Appropriate energy-harvesting (EH) mechanisms are required to convert these energy sources into electrical energy [5]. Piezoelectric device (PD) is an excellent candidate for harvesting electrical energy from ambient vibrations [6], [7], [8], which is one of the most commonly available energy sources.

Apart from the material itself [9], the research and development of a piezoelectric energy harvesting (PEH) system encompass three main aspects, namely, mechanical system [10], electronic circuit and storage device. A flow chart summarising the main function of these aspects in the PEH process is shown in Fig. 1.

A PD is often mechanically attached to a simple mechanical structure, such as a metallic cantilever beam to increase its EH efficiency [11], [12], [13]. When this EH system is subjected to mechanical vibration, the PD generates electricity under the converse piezoelectric effect. The electricity generated can be used to power electronic devices (load) or be stored in storage devices such as batteries for later use. The electrical energy harvested from PD is in micro-scale, which can be used for powering remote sensors for structural health-monitoring (SHM) purposes [14], [15], for powering medical devices [16], for feeding loads in military [17], for

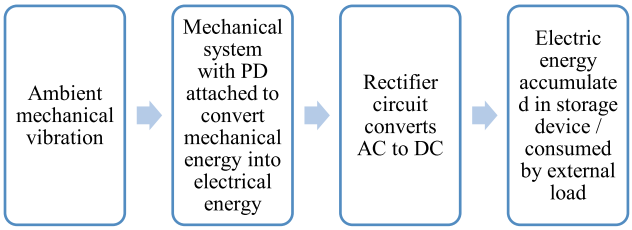

FIGURE 1. A flow chart summarising the PEH process.

powering cameras for animal tracking [18], and for charging mobile phones [19].

Electrically, a vibrating PD behaves as a capacitive AC source [20]. It needs to be converted to direct current (DC) for practical use. Therefore, an electronic rectifier circuit, known as the AC-DC rectifier circuit, is needed for the conversion. A traditional full-wave bridge rectifier (FBR) circuit serves the purpose, but it suffers from one major drawback – high power loss due to its forward voltage [4], [5], [21], [22], [23], [24], [25]. In addition, to operate the FBR circuit, the voltage generated by the PD, V_{PD} must be higher than the diode's forward voltage, which is expressed as:

$$V_{PD} > V_{rect} + 2V_D \tag{1}$$

Where V_{rect} is the output voltage of rectifier, and V_D is the voltage drop. If Eq. (1) is not satisfied, the voltage generated by the PD is internally dissipated, resulting in loss of energy. An efficient AC-DC rectifier circuit is therefore highly sought after to minimise energy loss.

For the FBR circuit, maximum rectified voltage occurs under no-load condition [26], [27], [28], and it is ideally equal to the peak – peak open circuit voltage at the PD terminals [29]. When the peak-peak voltage of PD is lower than the diode's forward voltage, the rectifier circuit is non-operational. To overcome these drawbacks, numerous rectifier circuits have been previously proposed for PEH.

Another commonly used traditional rectifier circuit is voltage doubler (VD) [20], [27], [30], [31]. Similarly, due to high forward voltage of the diodes used in the circuit, it is also not ideal for PEH. This is particularly concerning at high frequency of excitation, as the voltage generated is relatively small. The use of these circuits could lead to loss of voltage and subsequently result in high conversion loss and low efficiency [32].

Several strategies have been proposed by various researchers in this field to reduce power loss due to the presence of diodes. One example is the use of low-voltage drop Schottky diodes. However, this diode suffers from another drawback, which is its high reverse leakage current. When it is in reverse bias mode, current flows through the depletion region, resulting in dissipation of power in the form of heat [19], [21], [32]. On the other hand, Devi *et al.* [33] proposed the use of zero-bias Schottky diodes with low forward voltage and rapid switching function. Ideally, this diode allows unidirectional current flow. However, reverse leakage remains a problem. The circuit itself is also very complex.

Lam *et al.* [34] proposed the use of active diodes in an attempt to tackle the drawbacks of semiconductor devices. This is particularly common in the field of wireless transmission and medicine. An active diode is a comparator-controlled switch, which replaces the junction-based diode. Due to its low forward voltage, significant improvement in the output power was achieved. However, the circuit was complex and costly. Another study by Bowers and Arnold [35] explored the possibility of combining a synchronised rectifier with an active diode for PEH. However, this method also suffers from high voltage loss due to high threshold voltage of the semiconductor devices.

A metal-oxide-semiconductor field-effect transistor (MOSFET) bridge rectifier circuit was proposed by [36] to eliminate the loss of voltage in diodes. A severe drawback of this circuit is the need of external power source to trigger the MOSFETs, which is inefficient and oftentimes impossible in practical applications. Another recent study was conducted on the MOSFET based rectifier circuit by Arul *et al.* [37] to reduce the power loss in the rectification process. A significant improvement in output power and efficiency was demonstrated when compared to the FBR circuit. However, the power conversion from the PD was still limited due to its high threshold voltage. The input voltage from the PD is 2.09 V, and this circuit does not commence operation if voltage is less than 0.5 V.

To overcome the abovementioned shortcomings, some researchers have proposed switching methods [20], [38], [39], [40]. However, the proposed switching circuits require additional components such as inductors, switches, external power supply, polarity detectors and logic gates which renders the circuits complex and costly. More importantly, all the abovementioned circuits are non-operational in a low voltage environment (i.e., less than 0.3 V). Since the conventional diode forward voltage is 0.7 V, Eq. (1) is not satisfied. Therefore, the voltage generated by the PD is often internally wasted. Even it is partially satisfied, most of the energy is wasted. Thus, the power efficiency of such circuits is very low.

To overcome this drawback, a MOSFET rectifier circuit was used in [41]. Significant improvement in power conversion was demonstrated. However, the proposed full-bridge MOSFET rectifier circuit with switching method (Fig. 2) includes additional components, namely, a large inductor and the use of PWM technique, which make the circuit rather complex and costly. The study also did not discuss appropriate electrical boundary conditions.

The abovementioned circuit is later improved [41] by introducing an active MOSFET energy harvesting circuit (Fig. 3). Further improvement in power conversion, up to five times of the conventional rectifier circuit, was achieved.

However, this circuit is very complex due to additional components such as an inductor, switches, analog to digital

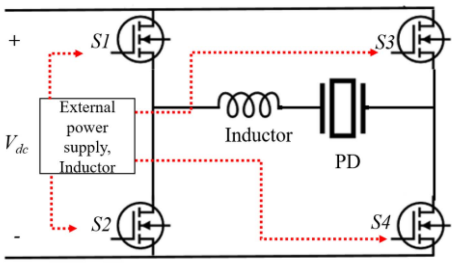

FIGURE 2. Full-bridge MOSFET Circuit with Switching Method.

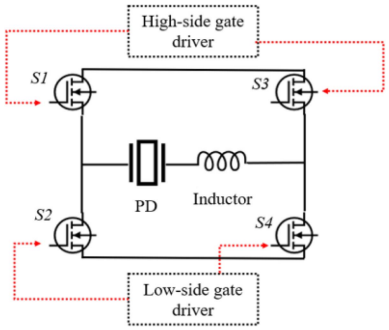

FIGURE 3. Active MOSFET Energy Harvesting Circuit.

converters, peak detector, logic gates, resulting in high cost. In addition, the additional components consume power up to 1 mW. High voltage is also required to kick start both circuits (Fig. 2 and Fig. 3). This is almost unachievable at a high frequency excitation, as the voltage produced is rather low.

Therefore, there is a need to design a more efficient circuit which could convert AC-DC with minimal complexity, without the need of external power supply, and has the capability of conversion even when the input voltage is low. In addition, previous studies mainly focused on PEH with rather high input voltage (2 – 5 V) at a high frequency of excitation (i.e., $>$ 100 Hz).

Some real-life examples of such high frequency vibrations include car engine compartment, cloth dryer, casing of kitchen blender, air noise, power converters and subwoofer. The PD can only generate a few micro or milliwatts of power under such high frequency of vibrations, which cannot satisfy Eq. (1) [35], [36], [37], [42], [43], [44].

To overcome the above issues, a modified self-driven H-Bridge AC-DC rectifier circuit, consisting of MOSFETs, is proposed in this article. An attempt is made to circumvent the problem of power loss in diodes and to reduce the complexity of the circuit. The need of external power source is also eliminated. Due to the low threshold voltage of MOSFETs, improvement in the output power is anticipated as a result of lower loss. In addition, the cost of this circuit is expected to reduce due to lower complexity. Key differences between the proposed circuit and existing circuits are:

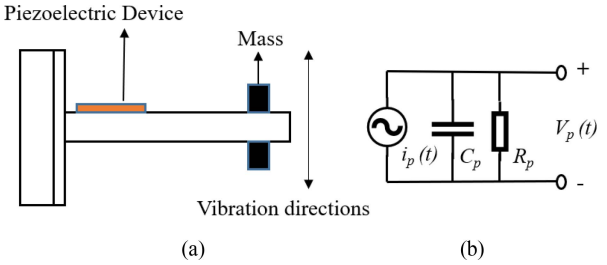

FIGURE 4. (a) A vibrating PD (left), (b) PD equivalent circuit model (right).

1. The proposed circuit does not require extra components such as an inductor, polarity detector, which renders the circuit less complicated, and thus lower cost.
2. Another distinct advantage is that it does not require an external power supply to trigger the MOSFET.
3. The use of MOSFETs includes a parasitic diode, which protects the proposed circuit from reverse voltage polarity, effectively lowering the power loss [45], [46].
4. The proposed circuit is expected to turn-on at very low voltage (0.28 V), i.e., it satisfies Eq. (1) easily.
5. This circuit is expected to function at high and low frequency ranges.

A series of experimental tests were conducted in this study to investigate the performance of the proposed H-Bridge rectifier circuit, in terms of output voltage, output power and efficiency over both high and low frequency ranges.

II. EQUIVALENT CIRCUIT MODEL OF PIEZOELECTRIC ENERGY HARVESTER AND AC-DC RECTIFIER CIRCUITS

This section presents a series of literature reviews, starting from the equivalent circuit modelling of a PEH system, followed by a review of conventional FBR circuit and VD commonly used for AC-DC rectification. The proposed H-Bridge rectifier circuit is then introduced.

A. EQUIVALENT CIRCUIT MODEL OF PIEZOELECTRIC ENERGY HARVESTER

From an electrical point of view, a harmonically vibrating PD can be modelled as a sinusoidal current source, $i_p(t)$ connected in parallel to its internal capacitance, $C_p$and its internal resistance, R_p [5], [20]. Fig. 4(a) and 4(b) illustrates a physical PD and its equivalent circuit model, respectively. The sinusoidal current source, $i_p(t)$ is expressed as:

$$i_P(t) = \widehat{I_p} sin(\omega t) \tag{2}$$

where $\widehat{I_P}$ is the magnitude of the sinusoidal current, ω is the angular frequency and t is time [29]. Alternatively, the vibrating PD can also be represented by an equivalent circuit consisting of a voltage source connected in series with a capacitance [29]. The AC generated by the PD varies with the amplitude and the frequency of the vibration source, but it is assumed relatively constant, regardless of external loading [47].

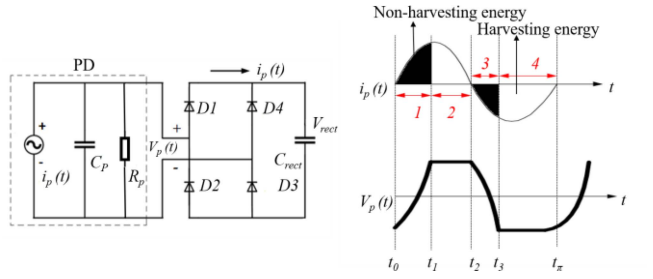

FIGURE 5. (a) A PD connected in parallel to an FBR circuit, (b) Current and voltage waveforms generated by FBR circuit (shaded portion indicates energy loss).

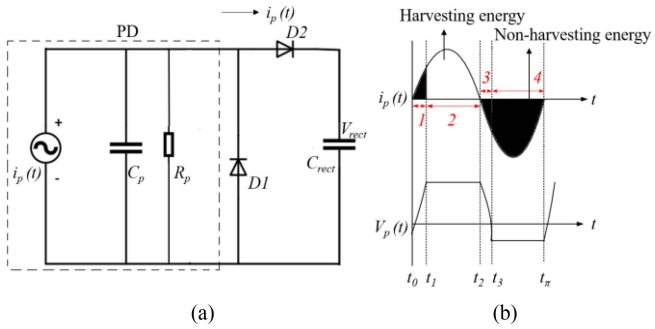

FIGURE 6. (a) A PD connected to VD and (b) current and voltage waveforms generated by the PD.

B. FBR CIRCUIT

The FBR circuit comprises of four diodes and is usually connected in parallel to the PD as shown in Fig. 5(a). The current and the voltage waveforms generated by the PD after rectification by the FBR circuit are shown in Fig. 5(b). As stated in *Section II-A*, the current, $i_p(t)$, generated by the PD will first charge and discharge the internal capacitance, C_p from $-(V_{rect} + 2V_D)$ to $(V_{rect} + 2V_D)$. This process occurs in both half cycles.

Taking the positive half cycle as example and referring to the rectified current waveform in Fig. 5(b), the current generated across Interval 1, known as the polarisation current, is used to charge the internal electrode capacitance of the PD. Thus, all the diodes are reverse biased, and there is no current output by the FBR circuit. When the time reaches t_1, the magnitude of the PD voltage, $V_P(t)$ is equal to the output voltage, V_{rect}. Within this interval, indicated as Interval 2 in Fig. 5(b), the output current flows to the DC filter capacitor, C_{rect}. In other words, energy is lost across Interval 1 (known as "*Non-harvesting energy*"), shown as shaded area in Fig. 5(b); whilst energy is generated across Interval 2 (known as "*Harvesting energy*"), shown as unshaded area. The circuit operation in both the positive and negative half cycles is summarised below:

B.1. POSITIVE HALF CYCLE

When $t_0 < t \leq t_1$ (Interval 1):

- PD charges or discharges its internal capacitor, C_P
- D1, D2, D3, D4: OFF

When $t_1 < t \leq t_2$ (Interval 2):

- PD delivers power to the capacitor, C_{rect}
- D1: ON, D3: ON
- $V_P(t) = V_{rect}$

B.2. NEGATIVE HALF CYCLE

When $t_2 < t \leq t_3$ (Interval 3):

- PD charges or discharges its internal capacitor, C_P
- D1, D2, D3, D4: OFF

When $t_3 < t = t_\pi$ (Interval 4):

- PD delivers power to the capacitor, C_{rect}
- D4: ON, D2: ON
- $V_P(t) = V_{rect}$

During both positive and negative half cycles, when the diodes are in turn-on condition, the output current flows into the capacitor, C_{rect}. When the DC filter capacitor load is connected in parallel to the rectifier circuit, maximum voltage is limited to the filter voltage [29], [45]. The output power varies with the output voltage, V_{rect} and the peak output power [48] occurs when:

$$V_{rect} = \frac{\widehat{I_p}(t)}{2\omega C_P} \tag{3}$$

and the charge produced by the PD in both positive and negative half cycle, Q_{total} is

$$Q_{total} = 2C_P V_P(t) \tag{4}$$

C. VD

Fig. 6(a) illustrates a circuit representation of a PD connected in parallel to a *VD* and a capacitor, C_{rect}. Its corresponding current, $i_p(t)$ and voltage, $V_p(t)$ waveforms are depicted in Fig. 6(b). Similar to the situation explained in *Section II-B* when $V_p(t)$ is less than V_{rect}, the diodes are in OFF condition. When $V_p(t)$ is equal to V_{rect}, the *VD* starts conducting. In the positive half cycle, the capacitor, C_{rect} is charged. However, in the negative half cycle, the current will flow to the ground. Thus, there is no output current.

In short, throughout Interval 1 and 3 (Fig. 6b), the internal capacitance of the PD is charged in both positive and negative half cycles, respectively. However, in Interval 2 and 4, which are the conduction period of the diodes in positive and negative half cycles, the capacitor, C_{rect} is only charged across Interval 2 but not Interval 4. Similar to the previous section, the shaded portions indicate non-harvesting energy, whereas the non-shaded portions represent harvesting energy.

Experimentally, this phenomenon has been demonstrated in [26]. The *VD* fails to provide any output current to the external load during the negative half cycle, so there is no output power. The process of energy accumulation in the capacitor throughout both half cycles are summarised as follows:

C.1. POSITIVE HALF CYCLE

When $t_0 < t \leq t_1$ (Interval 1):

- PD charges or discharges its internal capacitor, C_P
- D1, D2: OFF

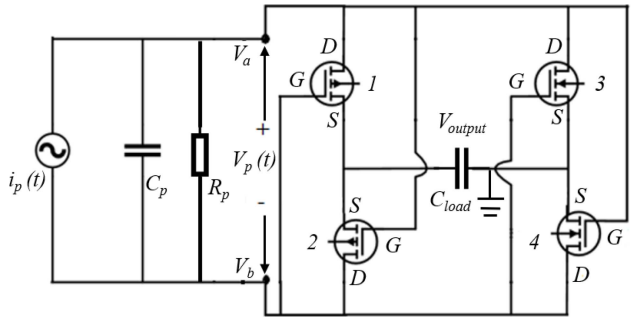

FIGURE 7. **Proposed H-Bridge rectifier circuit with MOSFETs connected to PD. (*1: M1-PMOS, 2: M2-PMOS, 3: M3-NMOS, 4: M4-NMOS, G: Gate, D: drain, S: source terminals*).**

When $t_1 < t \leq t_2$ (Interval 2):

- PD delivers power to the capacitor, C_{rect}
- D2: ON, D1: OFF
- $V_p(t) = V_{rect}$

C.2. NEGATIVE HALF CYCLE

When $t_2 < t \leq t_\pi$ (Interval 3, 4):

- PD does not deliver power to the capacitor, C_{rect}
- D1: OFF, D2: OFF
- No output flows to C_{rect}

Considering the VD fails to convert any voltage and current in the negative half cycle from the PD, it is deemed ineffective when compared to the FBR circuit. Thus, VD is not experimentally investigated in this study.

D. PROPOSED H-BRIDGE RECTIFIER CIRCUIT

In this study, an H-Bridge rectifier circuit, as shown in Fig. 7 was designed using MOSFETs (Threshold voltage = 0.3V) in order to minimise the conduction drop. This leads to higher conversion capability and thus, higher power conversion [49]. Another distinct advantage of the proposed rectifier circuit is that it does not require external power to drive its gate terminals.

It is worth mentioning that, the key difference between a traditional diode and a MOSFET with respect to their terminals is that the diode has two terminals, namely, anode and cathode; while MOSFET has three-terminals, namely, gate (G), drain (D), and source (S).

The MOSFET is a controlled device, i.e., the output current can be controlled by varying the voltage on the gate terminal. It has no gate diode, and it is possible to operate with both positive or negative voltage. Since the MOSFET has three terminals, it can be used for flowing current in both directions (D $\leftrightarrow$ S). On the other hand, the diode only has anode and cathode terminals, which is a unidirectional device. In spite of the abovementioned advantage, the design of MOSFET is relatively complex when compared to a diode.

The MOSFETs operate in two modes, namely, depletion mode and enhancement mode. In the depletion mode, the MOSFET functions like a normally closed switch, in which current can flow through when no voltage is applied. On the other hand, applying a negative voltage would cause a negative current flow to stop. In the enhancement mode, the MOSFET functions as a variable resistor (i.e., N-channel or P-channel). To turn on these MOSFETs, it is necessary to apply a threshold voltage to the gate terminal as the positive threshold voltage for N-Channel, and a negative voltage for P-Channel [28]. The MOSFET starts working, the On-resistance of MOSFET, $R_{DS(On)}$ is:

$$R_{DS(on)} = \frac{V_{DS}}{I_D} \tag{5}$$

where V_{DS} is drain - source voltage, and, I_D is drain current.

When the H-Bridge rectifier circuit is connected to the vibrating PD, it first charges the internal capacitor, C_p of the PD. When the internal capacitor is charged, the AC will be delivered to the H-Bridge rectifier circuit. The operation of the charging of output capacitor throughout both half cycles are summarised as follows:

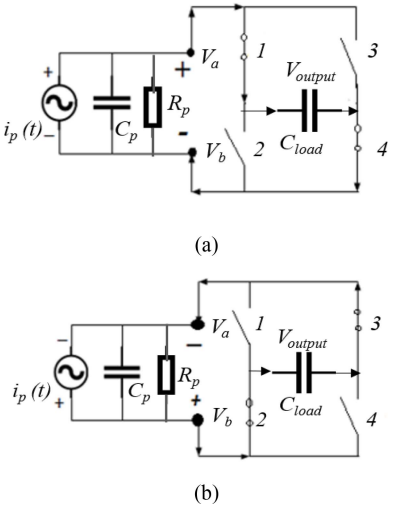

FIGURE 8. **Equivalent circuit of the proposed H-Bridge rectifier circuit in (a) positive half cycle, and (b) negative half cycle.**

D.1. POSITIVE HALF CYCLE

Fig. 8(a) shows the equivalent circuit of the proposed H-Bridge rectifier circuit when operating in the positive half cycle. During this cycle, the current will charge and discharge the internal capacitance, C_p of the PD when the voltage generated by the PD, $V_p(t) \leq V_{output}$, in which V_{output} is the rectified output voltage.

On the other hand, when $V_p(t) \geq V_{output}$, the H-Bridge rectifier circuit starts to conduct. At this time, M1-PMOS and M4-NMOS transistors are in conduction mode. Thus, the rectified voltage is stored in a load capacitor, C_{load}.

D.2. NEGATIVE HALF CYCLE

Fig. 8(b) shows the equivalent circuit of the H-Bridge rectifier circuit when operating in the negative half cycle.

TABLE 1. Testing scenario of test 1 (varying input voltage - constant frequency).

Scenario	Peak voltage of PD (V_{Pk})	Input current (μA)	Frequency (Hz)	Rectifier circuits	Storage capacitors (μF)
Test 1	0.28 0.42 0.56 0.70	4.8 7.3 10.1 13.1	100	*H-Bridge* *FBRLow* *FBRHigh*	C1 = 1 C2 = 10 C3 = 100

Similarly, when $V_p(t) \geq V_{output}$, it starts to conduct. At this time, M2-PMOS and M3-NMOS transistors are in conduction mode. Thus, the rectified voltage is stored in a load capacitor, C_{load}. The parasitic capacitance of MOSFET between the terminals can affect the performance of the circuit. Power loss also occurs during the switching period, knowns as the switching losses. Therefore the switching loss, $P_{switchingloss}$, of the MOSFET can be expressed as:

$$P_{switching\ loss} = \frac{1}{2} V_{DS} I_D \left(t_{on} + t_{off}\right) \tag{6}$$

where t_{on}, t_{off} are the turn on and off timings of the MOSFET respectively.

Power and efficiency are useful indicators of the performance of rectifier circuits. In this study, these parameters are used to compare the performance of various rectifier circuits. To find the efficiency, both input power and output power should first be calculated.

The input power, P_i is expressed as:

$$P_i = \frac{V_{Pk}}{\sqrt{2}} \cdot \frac{I_{Pk}}{\sqrt{2}} cos\varphi \tag{7}$$

where V_{Pk} and I_{Pk} are the peak voltage amplitude and current, respectively of PD. φ is the phase angle between the voltage and the current of PD. On the other hand, the power output by the rectifier circuits, P_o is calculated through the product of the output voltage, V_o and the output current, I_o through the capacitor, then the efficiency can be calculated [50].

III. EXPERIMENTAL VERIFICATION

The performance of the proposed H-Bridge rectifier circuit was experimentally investigated using two test setups: 1) at high excitation frequency (Test 1 & Test 2), and 2) at low excitation frequency (Test 3).

In Test 1, the power extracted from the PD through different rectifier circuits and capacitors under varying input voltages and constant frequency was investigated. Details are summarised in Table 1.

In Test 2, the power extracted from the PD through different rectifier circuits and capacitors under varying excitation frequency and constant input voltage was investigated. Details are summarised in Table 2.

In Test 3, the performance of the proposed circuit at low frequency of excitation was studied using the finger tapping method.

TABLE 2. Testing scenarios of test 2 (varying frequencies, constant voltage).

Scenario	Frequency (Hz)	Output current I_i (μA)	Peak Voltage (V_{Pk})	Rectifier circuits	Storage capacitors (μF)
Test 2	110 120 130 140	9.6 10.4 12.2 12.7	0.7	*H-Bridge* *FBRLow* *FBRHigh*	C1 = 1 C2 = 10 C3 = 100

In order to compare the performance of the proposed H-Bridge rectifier circuit, the comparison is made with the conventional FBR circuits. The details of each rectifier circuit adopted in this study are listed as follows:

a) FBR circuit with low forward voltage diodes (IN5820 AHIM, forward voltage, $V_f = 0.15$ V), denoted as *FBRLow*
b) FBR circuit with standard forward voltage diodes (IN4007, forward voltage, $V_f = 0.55$ V), denoted as *FBRHigh*
c) H-Bridge rectifier circuit with low threshold voltage MOSFETs (threshold voltage, $V_{th} = 0.3$ V, RZR040P01 – PMOS, AP2306AGN – NMOS), denoted as *H-Bridge*.

The abovementioned forward voltage of the diodes was also checked and verified using a voltmeter.

Fig. 9 shows the general experimental setup and procedures to study the performance of the *H-Bridge* and *FBR circuits* in Test 1, 2.

The main criteria for choosing components in the rectifier circuit is based on the voltage generated by the PD. In this study, the range of voltage generated by the PD is from 0.2 to 0.5 V_{rms}. Therefore, MOSFETs, with a threshold of 0.3V, is chosen for the H-Bridge circuit. For comparison with conventional FBR circuit, a commonly used diode with 0.55V and another one with 0.15 V was chosen.

The performance of the circuits was experimentally tested by connecting them to a PD attached to an aluminium beam. A mechanical shaker was used to generate controlled vibrations to the aluminium beam, which in turns excite the PD.

A macrofibre composite (MFC) patch, (type: M2814-P2, dimension: 37 mm x 17 mm x 0.180 mm, internal capacitance: 30.79nF) was used as PD in this experiment. The MFC patch was surfaced-bonded to one end of a lab-sized aluminium beam (dimension: 205 mm x 20 mm x 1 mm). This end of the beam was then fixed to a mechanical shaker. The other end of cantilever beam carried two permanent magnets. The two permanent magnets were placed at the tip of the cantilever beam, one on the top surface and the other on the bottom surface. The magnets were configured such that they are attracting each other. Since they are very strong magnets, such configuration resembles firmly attaching a proof mass at the tip of the cantilever. A permanent magnet was used for the sake of convenience in changing tip mass, such that the cantilever beam can be easily reused for different tests. These magnets, acting as proof mass, reduce the resonance

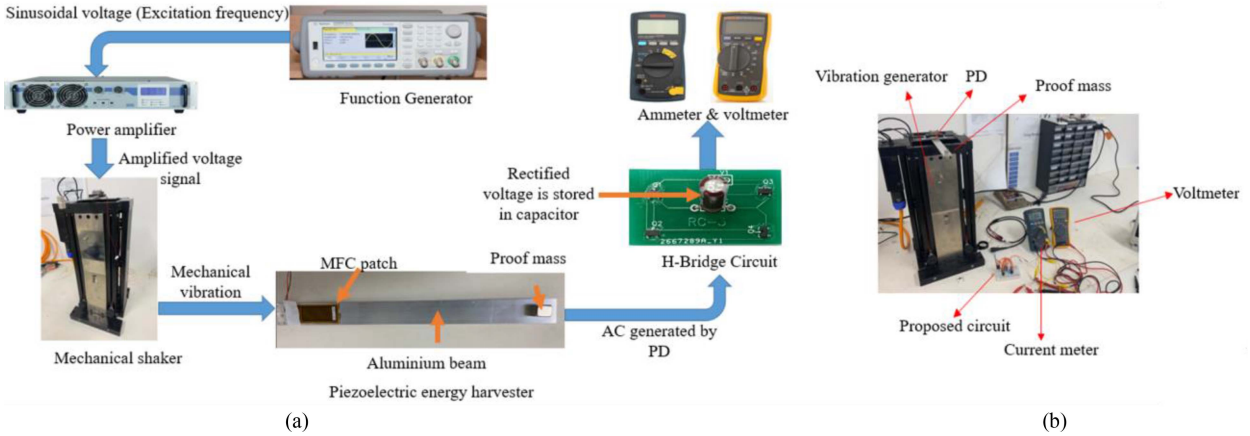

FIGURE 9. **(a) Flow chart illustrating the experimental process, (b) Experimental setup.**

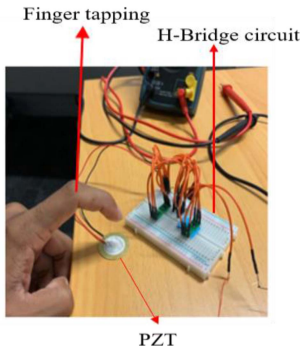

FIGURE 10. **Experiment of Test 3.**

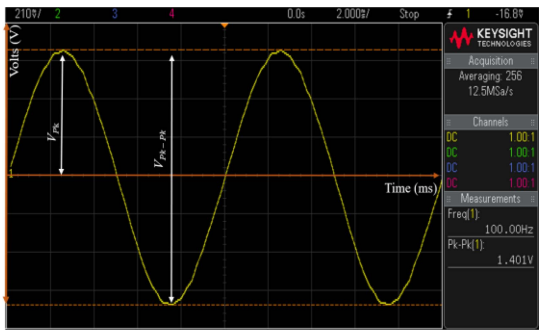

FIGURE 11. **The waveform generated by the piezoelectric device in Test 1.**

frequency of the cantilever beam, as well as increase the displacement at the free end [11].

A function generator (Agilent 33210A) was used to provide a sinusoidal signal of specified frequency to a power amplifier (2706, B & K Agilent), which then amplified the signal before activating the mechanical shaker (APS-113). The shaker generated mechanical vibrations according to the input frequency to excite the cantilever beam with attached PD. When the PD was subjected to excitation, it generated AC.

The open circuit voltage of PD was measured by a voltmeter, FLUKE 115, and the current was measured by a current meter, CD771. Besides, the voltage waveform of the PD was also observed in the oscilloscope.

In Test 3, the performance of *H-Bridge* was tested at low frequency. Another distinct type of piezoelectric device, namely PZT (Lead Zirconate Titanate) is employed. Fig. 10 shows the experimental setup of the proposed circuit in parallel with a PZT patch (25 mm in diameter), which acts as an input voltage source. This experiment was conducted only on *H-Bridge* as the main focus is on high frequency vibration.

To generate low frequency vibration, the finger tapping method is adopted as shown in Fig. 10. When mechanical pressured was applied, it generated AC which is sent to *H-Bridge* for rectification. The rectified DC voltage was stored in a ceramic capacitor of 1 μF. The voltage and current across the capacitor was similarly measured to calculate the output power.

A. TEST 1: VARYING INPUT VOLTAGE AT CONSTANT FREQUENCY

In Test 1, the frequency was kept constant at 100 Hz while the amplitude of the input voltage was varied. For each case, three storage capacitors (C1, C2 and C3) were tested.

The amplitude of the voltage was adjusted using the power amplifier to obtain the desired peak open circuit voltages. The measured peak voltage, V_{Pk} of PD was shown in Table 1. The input power were calculated using the Eq. (7).

One of the waveforms captured by the oscilloscope at 100Hz and peak voltage of 0.70 V is shown in Fig. 11.

When the measured open circuit voltages of PD are 0.28 V,0.42 V, 0.56 V and 0.70 V, the rectified voltage from *H-Bridge* and *FBRLow* circuits is shown in Fig. 12 (a).

Note that the rectified voltage of *FBRHigh* is not shown as the rectified voltage is too low (due to its high forward voltage) and is thus neglected. The corresponding calculated output power from the PD were 0.44 μW, 1.0 μW, 2.0 μW, and 3.2 μW, as depicted in Fig. 12 (b).

The power output by PD was applied to *H-Bridge* independently, and the rectified voltage was stored in an electrolytic capacitors (details tabulated in Table 1).

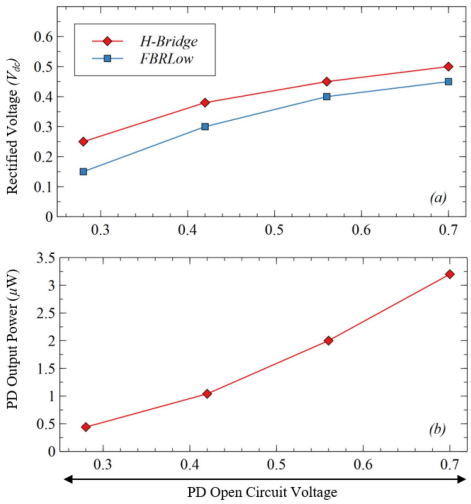

FIGURE 12. **(a) The rectified voltage of circuits and (b) the output power of PD in Test 1.**

Then the power output from *H-Bridge* was calculated by taking the product of voltage and current measured across the capacitor. Similarly, the output power of *FBRLow* and *FBRHigh* were also calculated. The output against input power for different circuits and capacitors are graphically presented in Fig. 13. The *FBRLow* curve shows that the rectified output voltage is around half of the PD's open circuit peak voltage. On the other hand, the rectified output voltage from the *H-Bridge* circuit is consistently higher than the *FBRLow* circuit.

When the input power of 0.44 μW was applied to the *H-Bridge*, 0.27 μW of output power was generated and stored in capacitor C1, as shown in Fig. 13(a). Similarly, with the same input power, rectification through *FBRLow* and *FBRHigh* produced 0.20 μW and 0 μW, respectively. In this particular case, the *H-Bridge* outperformed the two *FBR circuits*. Observing other cases of different input power and capacitors, it is found that the use of *H-Bridge* consistently yield the highest output power, in comparison to the *FBR circuits*. This is particularly true when larger capacitors (C2 and C3) are used. This demonstrates that the *H-Bridge* is superior to the FBR counterparts.

It is also noted that the *FBRHigh* curve produced zero power when the voltage is low ($<$ 0.42 V), as a result of its high forward voltage. In general, if the forward voltage is not zero or ideal, its behaviour differs from the actual characteristics of the diode. The key difference between an ideal diode and a standard diode is current consumption. Consequently, the power produced is significantly lesser than both *H-Bridge* and *FBRLow* circuits.

The main reason causing both *FBRLow* and *FBRHigh* to yield lower output power is the use of diodes with high forward voltage. This problem is alleviated when *H-Bridge* is used. The use of MOSFETs, which include a parasitic body diode has a lower forward voltage than normal diodes.

The resistance path of MOSFET, which is from drain to source, is reduced with voltage is applied to the Gate terminal. Therefore, when sufficient input voltage is applied to *H-Bridge*, the conversion capability also increases.

To further understand the performance of the proposed circuit, a closer look is taken at the waveforms of the output voltage in oscilloscope (input voltage of 0.7 V) shown in Fig. 14. The rectified output voltage, V_o by *H-Bridge,* is represented by the green curve. The time required for charging the output capacitor is indicated as t_1 in the diagram. The interval between each "t_1" period is the discharging time of the output capacitor. The charging and discharging processes take place in both positive and negative half cycles.

As mentioned earlier, the MOSFETs are used to achieve higher voltage and efficiencies. They are rather straightforward due to fast switching. The power consumption is also low due to its low threshold voltage. As a result, the power converted by the proposed circuit is high, and the output capacitor is charged. The process is similar in the negative half cycle.

In the case of the *FBRLow*, the waveform of output voltage against time with 0.7 V of input voltage is represented by the red curve in Fig. 14. The charging period of the output capacitor is denoted as t_2. Similarly, interval between each t_2 period indicates the discharging time of the output capacitor. For each positive half cycle, the charging process starts when diodes D1 and D3 were turned ON. If the applied voltage is sufficient, *FBRLow* starts conducting, and the output capacitor will be charged. However, since the applied voltage is high, the resistance path from anode to cathode and the current consumption is also high. Therefore, the voltage output by *FBRLow* is relatively lower than the *H-Bridge*. In addition, the delay experienced by the *FBRLow* circuit is also longer than the *H-Bridge*.

The *FBRHigh* was tested under similar condition. The blue curve represents the waveform of its output voltage with 0.7 V of input voltage. In comparison to the *FBRLow*, the diodes used in the *FBRHigh* have even higher forward voltage, resulting in higher resistance in the circuit. Therefore, the power conversion is lower. The charging time of the output capacitor is unidentifiable and is thus not shown in Fig. 14.

B. TEST 2: VARYING FREQUENCY AT CONSTANT INPUT VOLTAGE

In Test 2, the performance of *H-Bridge* is studied under constant voltage at different frequencies. The frequencies applied are 110 Hz, 120 Hz, 130 Hz and 140 Hz. At each frequency, the peak open circuit voltage is adjusted and kept at 0.70 V. Note that due to the difference in frequencies, the current produced by the PD was different (Fig. 15). Therefore, the power applied to the circuits was also different. Each frequency was applied to all three circuits individually and the voltage rectified by the circuits was stored in electrolyte capacitors (acting as a load). Details are summarised in Table 2.

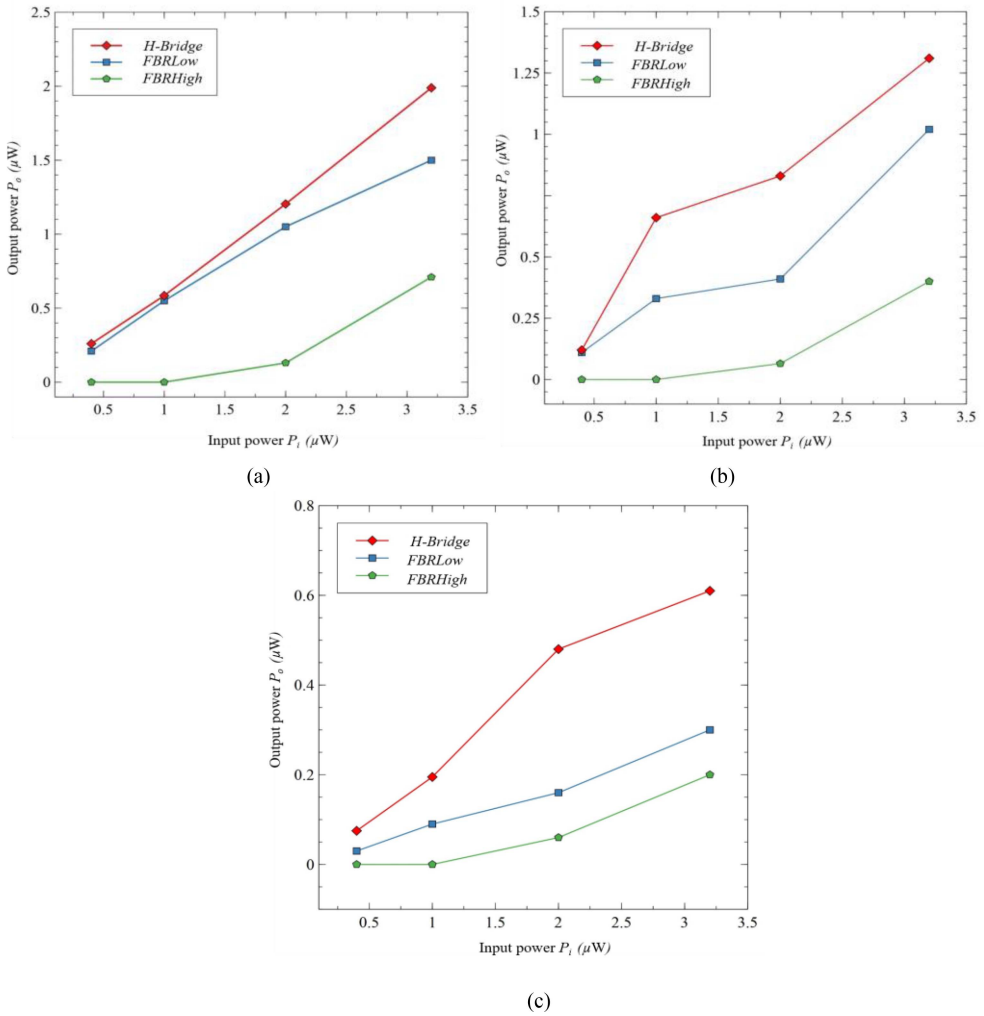

FIGURE 13. Power output by various rectifier circuits with varying input power with (a) Capacitor C1, (b) Capacitor C2, and (c) Capacitor C3 in Test 1.

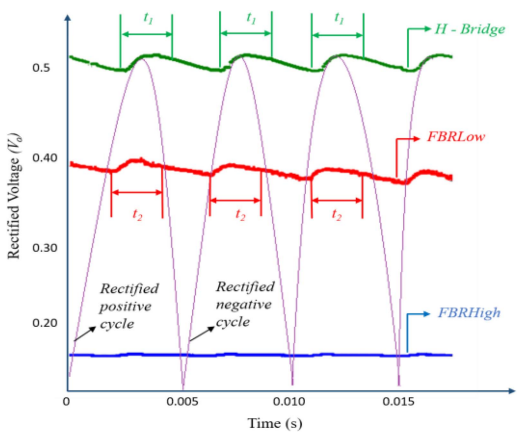

FIGURE 14. Waveform of voltage rectified by ***H-Bridge***, ***FBRLow***, and ***FBRHigh*** circuits in Test 1.

For each case, the voltage and current across the capacitor were measured with the voltmeter and ammeter. Similar to Test 1, they are used to calculate the output power.

In Test 2, the current produced by the PD at different frequencies with constant peak open circuit voltage of 0.7 V is in shown Fig. 15. The output current increases steadily with increase in frequency.

Fig. 16 shows the output power stored in capacitors C1, C2 and C3 under different frequency of excitation. The output power was calculated as the product of the output voltage and the output current through the capacitor. As an example, when an input power of 3.2 μW was applied to the *H-Bridge*, 2.01 μW of output power was generated and stored in capacitor C1.

It is noted that the power output through *H-Bridge* is consistently higher than its counterparts, regardless of the excitation frequency. It is also noted that the power extracted with larger capacitors is lower. This is attributed to the fact that larger capacitors possess higher capacitance and internal resistance, which reducesthe current (DC) through the capacitor.

By further inspecting Fig. 16, one could identify that the actuation frequency also affects the power converted by different rectifier circuits. This is especially obvious in the case

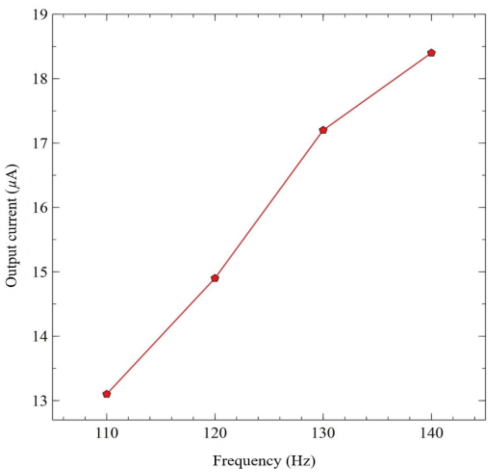

FIGURE 15. The output current waveform of PD when different frequencies were applied (Test 2).

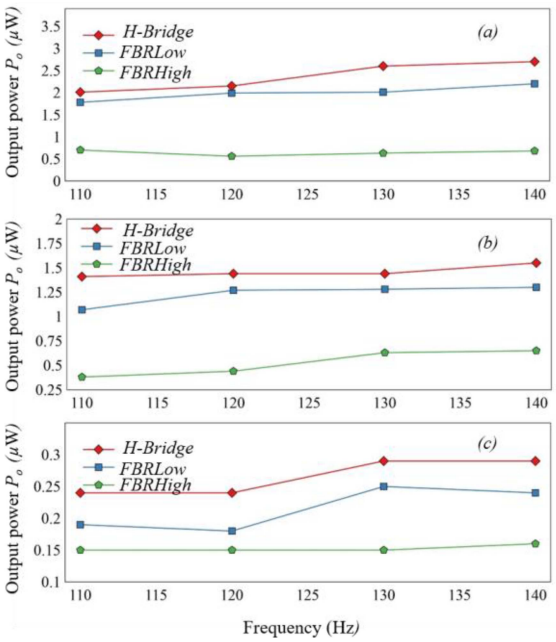

FIGURE 16. Power output by various rectifier circuits with varying input frequency through (a) Capacitor C1, (b) Capacitor C2, and (c) Capacitor C3 in Test 2.

of *H-Bridge*, in which the output power generally increases with the increase in frequency, despite the same input voltage of 0.7 V. This is mainly due to the fact that the current increases with increasing frequency.

However, the extent of increase in output power does not show consistent trend across different rectifier circuits, frequency ranges and capacitors. In the case of the FBR circuits, similar to Test 1, the power converted by *FBRLow* is always higher than *FBRHigh*, regardless of excitation frequency.

C. TEST 3: PERFORMANCE OF H-BRIDGE RECTIFIER CIRCUIT AT LOW FREQUENCY

To check the functionality of *H-Bridge* at low frequency, Test 3 was conducted using the finger tapping method.

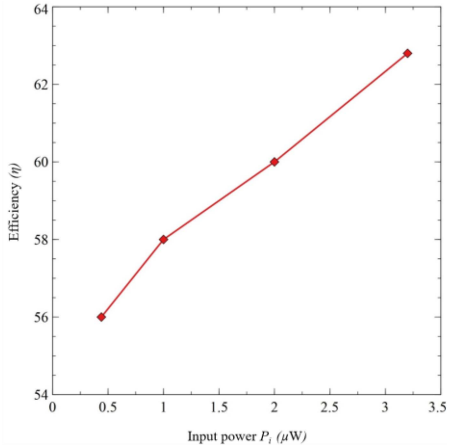

FIGURE 17. The efficiencies of *H-Bridge* in Test 1.

Considering the superiority of the H-Bridge circuit over the FBR circuits have been demonstrated in Test 1 and Test 2, the FBR circuits are not considered in Test 3.

In this test, when the voltage applied to *H-Bridge* by finger tapping was 0.68 V, the voltage rectified by *H-Bridge* was 0.53 V. The output power was calculated to be 1.90 μW. The voltage gain, V_a (ratio of output to input voltage of the circuit) of *H-Bridge* is calculated as 77.9%. An LED bulb was successfully powered with the rectified voltage. This simple experiment demonstrates the possibility of using the proposed *H-Bridge* circuit at low excitation frequency.

D. EFFICIENCY OF RECTIFIER CIRCUITS

In previous sections, it is demonstrated that the power extracted from the *H-Bridge* circuit is higher than the FBR circuits under Test 1 and Test 2. In this section, the efficiency of the *H-Bridge* and the *FBR circuits* are investigated. Comparison is also made with selected studies available in the literature. Fig. 17 shows the efficiency of the *H-Bridge* circuit against different input power based on Test 1. The efficiency of the circuit is found to increase steadily with the increase in input power.

The highest efficiency of 63% is achieved when the input power is 3.2 μW. This phenomenon can be explained by the fact that the MOSFETs are voltage-dependent. Therefore, the efficiency of the *H-Bridge* is initially low and it continuously increases with the increase in peak voltage of the PD.

For the sake of comparison, the efficiency of various circuits calculated from Test 1 and Test 2 are summarised in Fig. 18. Note that only the output obtained from Capacitor C1 is presented as those from Capacitors C2 and C3 show similar trend and is therefore omitted. Similar to the observation obtained from previous sections, the *H-Bridge* is found to yield higher efficiency than the *FBR* circuit counterparts under all testing conditions.

From Fig. 18(b), it can be observed that the efficiency of the *H-Bridge* circuit is rather stable with respect to changing frequency. This is mainly due to the fact that the voltage was kept constant at 0.7 V_{Pk} across different

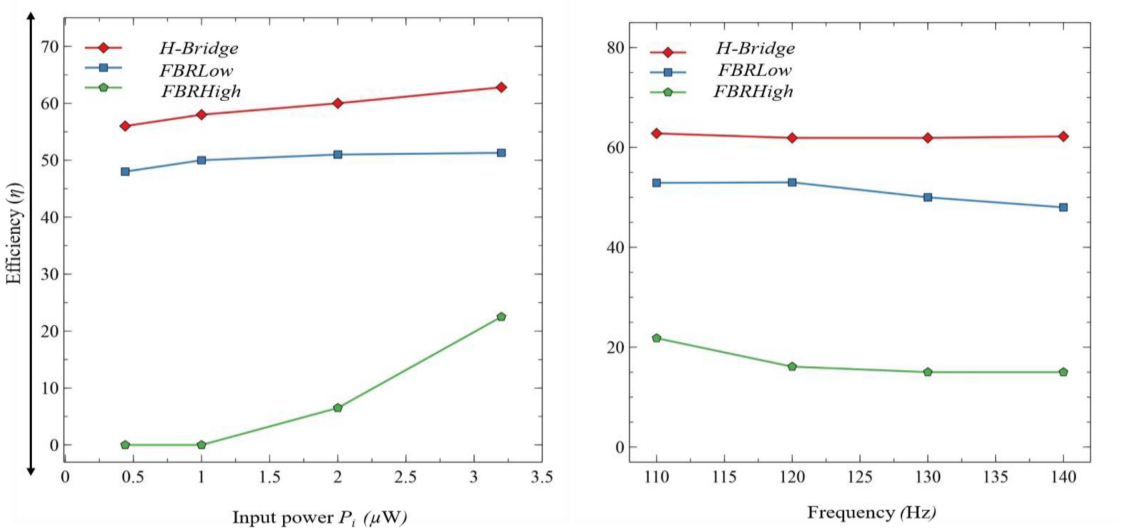

FIGURE 18. **The efficiency of *H-Bridge*, *FBRLow* and *FBRHigh* circuits connected to Capacitor C1 in (a) Test 1, and (b) Test 2.**

frequencies. Maximum efficiency achieved by the *H-Bridge* circuit is 62.8%, in comparison to 51% and 21.8% of *FBRLow* and *FBRHigh* circuits, respectively. The difference in performance is more pronounced at the higher frequency range. Therefore, it can be concluded that the diode-based FBR circuits are particularly inefficient when the input voltage is low and the excitation frequency is high. This is mainly due to its junction bias. With the use of the proposed *H-Bridge* circuit, the conversion loss in the semiconductor devices is effectively minimised.

For the sake of comparison, the conversion efficiency of various rectifier circuits published in previous studies is summarised in Table 3. The proposed *H-Bridge* stands out with a maximum efficiency of 63%, followed by Split capacitor conversion and Secondary diode conversion [51] of 60.3% and 57.4%, respectively. Maximum efficiency of the *FBRLow* and *FBRHigh* circuits investigated in this study are 51% and 22%, respectively. The *FBRHigh* circuit has similar efficiency as the AC-DC rectifier [37], which is expected.

It is worth mentioning that, in order to eliminate the forward voltage of the diodes, switching methods such as boost converter, secondary diode conversion and split capacitor conversion have been proposed by various researchers. However, the power loss associated with the use of switches is often high, resulting in relatively low efficiency [45], [47], [48]. It can thus be concluded that the proposed *H-Bridge* rectifier circuit demonstrates significant improvement in power conversion efficiency.

TABLE 3. **Performance comparison of various circuits available in the literature.**

Rectifier circuits	Peak voltage (V_{Pk})	Frequency (Hz)	Conversion efficiency (%)
AC-DC Rectifier [37]	2.18	200	38.08
MOSFET bridge rectifier [37]	2.09	200	44.8
A DC/DC boosting circuit [52]	0.12	Not provided	30
Standard energy conversion [53]	1	Not provided	51.43
Secondary diode conversion [54]	0.16	200	57.43
Split capacitor conversion [51]	0.4	200	60.3
Power-harvesting circuits [55]	0.3	Not provided	Not provided
FinFet inductive boost converter [56]	1.2	Not provided	Not provided
Proposed *H-Bridge* rectifier circuit	0.28 - 0.70	100 - 140	63
FBRLow	0.28 – 0.70	100 - 140	51
FBRHigh	0.28 – 0.70	100 – 140	22

IV. CONCLUSION

In this study, an improved, self-powered *H-Bridge* is proposed for AC-DC conversion of PEH system under low amplitude and high-frequency application. Taking advantage of MOSFETs as transistors, which possess low threshold voltage, the proposed rectifier circuit results in higher power conversion and higher efficiency, when compared to the conventional *FBR circuits*. The experimental results showed that the output power and efficiency of the *H-Bridge* rectifier circuit is consistently higher than the *FBR* circuits with different diodes under all testing scenarios. With an input power of 3.2 μW and input voltage of 0.7 V_{Pk}, the proposed rectifier circuit produced 2.01 μW of output power. Maximum efficiency achieved is 63%, which is significantly higher than the *FBR* circuits. In addition, its application at low frequency is

also briefly investigated. It was found that the voltage gain of *H-Bridge* circuit is 78%, with output power of 1.9 μW. For future work, it is recommended that the proposed circuit be applied to real-life scenarios. Deeper investigation into low frequency application, such as human motion is also anticipated.

REFERENCES

[1] G. Sebald, S. Pruvost, and D. Guyomar, "Energy harvesting based on Ericsson pyroelectric cycles in a relaxor ferroelectric ceramic," *Smart Mater. Struct.*, vol. 17, no. 1, 2007, Art. no. 015012.

[2] S. Roundy, P. K. Wright, and J. Rabaey, "A study of low level vibrations as a power source for wireless sensor nodes," *Comput. Commun.*, vol. 26, no. 11, pp. 1131–1144, 2003.

[3] A. M. D. Broe, S. Drouilhet, and V. Gevorgian, "A peak power tracker for small wind turbines in battery charging applications," *IEEE Trans. Energy Convers.*, vol. 14, no. 4, pp. 1630–1635, Dec. 1999.

[4] L. Garbuio, M. Lallart, D. Guyomar, C. Richard, and D. Audigier, "Mechanical energy harvester with ultralow threshold rectification based on SSHI nonlinear technique," *IEEE Trans. Ind. Electron.*, vol. 56, no. 4, pp. 1048–1056, Apr. 2009.

[5] A. Erturk and D. J. Inman, *Piezoelectric Energy Harvesting*. Chicester, U.K.: Wiley, 2011.

[6] Y.-C. Chang and C.-M. Liaw, "Design and control for a charge-regulated flyback switch-mode rectifier," *IEEE Trans. Power Electron.*, vol. 24, no. 1, pp. 59–74, Jan. 2009.

[7] T. T. Le, J. Han, A. von Jouanne, K. Mayaram, and T. S. Fiez, "Piezoelectric micro-power generation interface circuits," *IEEE J. Solid-State Circuits*, vol. 41, no. 6, pp. 1411–1420, Jun. 2006.

[8] I. Izadgoshasb, Y. Y. Lim, N. Lake, L. Tang, R. V. Padilla, and T. Kashiwao, "Optimizing orientation of piezoelectric cantilever beam for harvesting energy from human walking," *Energy Convers. Manag.*, vol. 161, pp. 66–73, Apr. 2018.

[9] U. B. A. Godse, *Basic Electronics Engineering*. Pune, India: Techn. Publ., 2008.

[10] I. Izadgoshasb, Y. Y. Lim, R. Vasquez Padilla, M. Sedighi, and J. P. Novak, "Performance enhancement of a multiresonant piezoelectric energy harvester for low frequency vibrations," *Energies*, vol. 12, no. 14, p. 2770, 2019.

[11] I. Izadgoshasb, Y. Y. Lim, L. Tang, R. V. Padilla, Z. S. Tang, and M. Sedighi, "Improving efficiency of piezoelectric based energy harvesting from human motions using double pendulum system," *Energy Convers. Manag.*, vol. 184, pp. 559–570, Mar. 2019.

[12] S. Roundy *et al.*, "Improving power output for vibration-based energy scavengers," *IEEE Pervasive Comput.*, vol. 4, no. 1, pp. 28–36, Jan.–Mar. 2005.

[13] J. Xu and J. Tang, "Multi-directional energy harvesting by piezoelectric cantilever-pendulum with internal resonance," *Appl. Phys. Lett.*, vol. 107, no. 21, 2015, Art. no. 213902.

[14] Z. S. Tang, Y. Y. Lim, S. T. Smith, and I. Izadgoshasb, "Development of analytical and numerical models for predicting the mechanical properties of structural adhesives under curing using the PZT-based wave propagation technique," *Mech. Syst. Signal Process.*, vol. 128, pp. 172–190, Aug. 2019.

[15] Y. Y. Lim, S. T. Smith, and C. K. Soh, "Wave propagation based monitoring of concrete curing using piezoelectric materials: Review and path forward," *NDT E Int.*, vol. 99, pp. 50–63, Oct. 2018.

[16] A. M. Eltamaly and K. E. Addoweesh, "A novel self-power SSHI circuit for piezoelectric energy harvester," *IEEE Trans. Power Electron.*, vol. 32, no. 10, pp. 7663–7673, Oct. 2017.

[17] R. Weigel *et al.*, "Microwave acoustic materials, devices, and applications," *IEEE Trans. Microw. Theory Techn.*, vol. 50, no. 3, pp. 738–749, Mar. 2002.

[18] Z. D. Deng *et al.*, "Transmitters for animals and methods for transmitting from animals," Google Patents US20 170 164 581 A1, 2017.

[19] M. Yuan, Z. Cao, and J. Luo, "Characterization the influences of diodes to piezoelectric energy harvester," *Int. J. Smart Nano Mater.*, vol. 9, no. 3, pp. 151–166, 2018.

[20] S. Lu and F. Boussaid, "A highly efficient P-SSHI rectifier for piezoelectric energy harvesting," *IEEE Trans. Power Electron.*, vol. 30, no. 10, pp. 5364–5369, Oct. 2015.

[21] S. Cheng, Y. Jin, Y. Rao, and D. P. Arnold, "A bridge voltage doubler AC/DC converter for low-voltage energy harvesting applications," in *Proc. PowerMEMS Conf.*, 2009, pp. 25–28.

[22] D. Guyomar and M. Lallart, "Recent progress in piezoelectric conversion and energy harvesting using nonlinear electronic interfaces and issues in small scale implementation," *Micromachines*, vol. 2, no. 2, pp. 274–294, 2011.

[23] N. A. A. Nawir, A. A. Basari, M. S. M. Saat, N. X. Yan, and S. Hashimoto, "A review on piezoelectric energy harvester and its power conditioning circuit," *ARPN J. Eng. Appl. Sci.*, vol. 13, no. 8, pp. 2993–3006, 2018.

[24] A. Shareef, W. L. Goh, S. Narasimalu, and Y. Gao, "A rectifier-less AC–DC interface circuit for ambient energy harvesting from low-voltage piezoelectric transducer array," *IEEE Trans. Power Electron.*, vol. 34, no. 2, pp. 1446–1457, Feb. 2019.

[25] F. Maiorca, F. Giusa, C. Trigona, B. Andò, A. R. Bulsara, and S. Baglio, "Diode-less mechanical H-Bridge rectifier for 'zero threshold' vibration energy harvesters," *Sens. Actuat. A, Phys.*, vol. 201, pp. 246–253, Oct. 2013.

[26] T. Kashiwao, I. Izadgoshasb, Y. Y. Lim, and M. Deguchi, "Optimization of rectifier circuits for a vibration energy harvesting system using a macro-fiber composite piezoelectric element," *Microelectron. J.*, vol. 54, pp. 109–115, Aug. 2016.

[27] A. Tabesh and L. G. Frechette, "An improved small-deflection electromechanical model for piezoelectric bending beam actuators and energy harvesters," *J. Micromech. Microeng.*, vol. 18, no. 10, 2008, Art. no. 104009.

[28] V. Subramanyam, *Power Electronics–Devices, Converters and Applications*, New Age Int. Publ. Pvt. Ltd., Bangalore, India, 2006.

[29] A. Tabesh and L. G. Frechette, "A low-power stand-alone adaptive circuit for harvesting energy from a piezoelectric micropower generator," *IEEE Trans. Ind. Electron.*, vol. 57, no. 3, pp. 840–849, Mar. 2010.

[30] Y. Hattori and Y. Hatano, "Power generating device and tire provided therewith," Google Patents US20 070 205 691 A1, 2008.

[31] Y. Wang and D. J. Inman, "A survey of control strategies for simultaneous vibration suppression and energy harvesting via piezoceramics," *J. Intell. Mater. Syst. Struct.*, vol. 23, no. 18, pp. 2021–2037, 2012.

[32] A. Bar-Lev, *Semiconductors and Electronic Devices*. Englewood Cliffs, NJ, USA: Prentice-Hall Int., 1984.

[33] K. K. A. Devi, N. M. Din, and C. K. Chakrabarty, "Optimization of the voltage doubler stages in an RF-DC convertor module for energy harvesting," *Circuits Syst.*, vol. 3, no. 3, p. 216, 2012.

[34] Y.-H. Lam, W.-H. Ki, and C.-Y. Tsui, "Integrated low-loss CMOS active rectifier for wirelessly powered devices," *IEEE Trans. Circuits Syst. II, Exp. Briefs*, vol. 53, no. 12, pp. 1378–1382, Dec. 2006.

[35] B. J. Bowers and D. P. Arnold, "Spherical, rolling magnet generators for passive energy harvesting from human motion," *J. Micromech. Microeng.*, vol. 19, no. 9, 2009, Art. no. 094008.

[36] J. Colomer-Farrarons, P. Miribel-Catala, A. Saiz-Vela, M. Puig-Vidal, and J. Samitier, "Power-conditioning circuitry for a self-powered system based on micro PZT generators in a 0.13-μm low-voltage low-power technology," *IEEE Trans. Ind. Electron.*, vol. 55, no. 9, pp. 3249–3257, Sep. 2008.

[37] A. Arul, A. Clarence, and E. R. Samuel, "Efficiency evaluation of a MOSFET bridge rectifier for powering LEDs using piezo-electric energy harvesting systems," *Automatika: èasopis za automatiku, mjerenje, elektroniku, raèunarstvo i komunikacije*, vol. 57, no. 2, pp. 329–336, 2017.

[38] S. Du, Y. Jia, C. Zhao, G. A. Amaratunga, and A. A. Seshia, "A nail-size piezoelectric energy harvesting system integrating a MEMS transducer and a CMOS SSHI circuit," *IEEE Sensors J.*, vol. 20, no. 1, pp. 277–285, Jan. 2020.

[39] K. Savarimuthu, R. Sankararajan, and S. Murugesan, "Design and implementation of piezoelectric energy harvesting circuit," *Circuit World*, vol. 43, no. 2, pp. 63–71, 2017.

[40] L. Yu, H. Wang, and A. Khaligh, "A discontinuous conduction mode single-stage step-up rectifier for low-voltage energy harvesting applications," *IEEE Trans. Power Electron.*, vol. 32, no. 8, pp. 6161–6169, Aug. 2017.

[41] Y. Liu, G. Tian, Y. Wang, J. Lin, Q. Zhang, and H. F. Hofmann, "Active piezoelectric energy harvesting: General principle and experimental demonstration," *J. Intell. Mater. Syst. Struct.*, vol. 20, no. 5, pp. 575–585, 2009.

[42] C. Peters, O. Kessling, F. Henrici, M. Ortmanns, and Y. Manoli, "CMOS integrated highly efficient full wave rectifier," in *Proc. IEEE Int. Symp. Circuits Syst.*, New Orleans, LA, USA, 2007, pp. 2415–2418.
[43] H. Li, C. Tian, and Z. D. Deng, "Energy harvesting from low frequency applications using piezoelectric materials," *Appl. Phys. Rev.*, vol. 1, no. 4, 2014, Art. no. 041301.
[44] M. F. B. Ab Rahman and S. L. Kok, "Investigation of useful ambient vibration sources for the application of energy harvesting," in *Proc. IEEE Student Conf. Res. Develop.*, Cyberjaya, Malaysia, 2011, pp. 391–396.
[45] S. Hashemi, M. Sawan, and Y. Savaria, "A novel low-drop CMOS active rectifier for RF-powered devices: Experimental results," *Microelectron. J.*, vol. 40, no. 11, pp. 1547–1554, 2009.
[46] P. Bimbhra and S. Kaur, *Power Electronics*. New Delhi, India: Khanna Publ., 2012.
[47] N. Sreelakshmi and C. R. Reshma, "Single stage bridgeless boost rectifier for low power applications," in *Proc. Int. Conf. Control Power Commun. Comput. Technol. (ICCPCCT)*, Kannur, India, 2018, pp. 323–329.
[48] G. K. Ottman, H. F. Hofmann, A. C. Bhatt, and G. A. Lesieutre, "Adaptive piezoelectric energy harvesting circuit for wireless remote power supply," *IEEE Trans. Power Electron.*, vol. 17, no. 5, pp. 669–676, Sep. 2002.
[49] Y. Lu and W.-H. Ki, "A 13.56 MHz CMOS active rectifier with switched-offset and compensated biasing for biomedical wireless power transfer systems," *IEEE Trans. Biomed. Circuits Syst.*, vol. 8, no. 3, pp. 334–344, Jun. 2014.
[50] J. Liang and W. Liao, "On the influence of transducer internal loss in piezoelectric energy harvesting with SSHI interface," *J. Intell. Mater. Syst. Struct.*, vol. 22, no. 5, pp. 503–512, 2011.
[51] S. Dwari, R. Dayal, L. Parsa, and K. N. Salama, "Efficient direct AC-to-DC converters for vibration-based low voltage energy harvesting," in *Proc. IEEE 34th Annu. Conf. Ind. Electron.*, Orlando, FL, USA, 2008, pp. 2320–2325.
[52] A. Richelli, S. Comensoli, and Z. M. Kovács-Vajna, "A DC/DC boosting technique and power management for ultralow-voltage energy harvesting applications," *IEEE Trans. Ind. Electron.*, vol. 59, no. 6, pp. 2701–2708, Jun. 2012.
[53] G. D. Szarka, B. H. Stark, and S. G. Burrow, "Review of power conditioning for kinetic energy harvesting systems," *IEEE Trans. Power Electron.*, vol. 27, no. 2, pp. 803–815, Feb. 2012.
[54] J. Dicken, P. D. Mitcheson, I. Stoianov, and E. M. Yeatman, "Power-extraction circuits for piezoelectric energy harvesters in miniature and low-power applications," *IEEE Trans. Power Electron.*, vol. 27, no. 11, pp. 4514–4529, Nov. 2012.
[55] T. K. Halvorsen, H. A. Hjortland, and T. S. Lande, "Power harvesting circuits in 90 nm CMOS," in *Proc. IEEE NORCHIP Conf.*, Tallinn, Estonia. 2008, pp. 154–157.
[56] M. Yasir and M. Hasan, "High performance compact FinFET based inductive boost converter," in *Proc. Int. Conf. Instrum. Meas. Circuits Syst. (IMCAS)*, 2014, pp. 15–17.

MAHESH EDLA was born in India, in 1993. He received the B.Tech. degree in electrical and electronics engineering from JNTUH, India, and the M.Sc degree in electrical and electronics engineering from Coventry University, U.K. He is currently pursuing the Ph.D. degree in electronics engineering with Southern Cross University, Australia. Also, he worked in the piezoelectric energy harvesting field with Coventry University for four months. His current research includes designing electronic circuits for the rectification process.

YEE YAN LIM received the Ph.D. degree in civil engineering from Nanyang Technological University, Singapore, in 2012. He is a Senior Lecturer and a Civil Engineering Course Coordinator with the School of Environment, Science and Engineering, Southern Cross University. His current research interests are smart materials-based structural health monitoring and energy harvesting.

MIKIO DEGUCHI received the master's degree from the Graduate School of Engineering, Kyoto University in 1985, and the Ph.D. degree in engineering from Kyoto University in 2003. After working with Mitsubishi Electric Corporation for about ten years, he was transferred to National Institute of Technology (KOSEN), Niihama College, where he is currently a Professor with the Department of Electronics and Control Engineering. His research interests include electronic measurement technology, electronic circuit application, and development of intelligent teaching materials.

RICARDO VASQUEZ PADILLA received the B.S. and M.Sc. degrees in ME, the Ph.D. degree, and the Doctoral degree from the Department of Chemical and Biomedical Engineering, University of South Florida in 2011. He is a Senior Lecturer and a Course Coordinator of the Bachelor in Mechanical Engineering with the School of Environment, Science and Engineering, Southern Cross University. Prior to that position, he worked as Research Fellow with CSIRO Energy Centre, Newcastle, from 2014 to 2016, and as Assistant Professor with Universidad Del Norte from 2011 to 2014. His research interests include modeling, optimization, mechanical design, economic analysis, and testing of thermo-mechanical systems. He is currently working on the design of solar gas phase receivers and self-tunable wind energy harvesters.

IMAN IZADGOSHASB received the Ph.D. degree in mechanical engineering from Southern Cross University, Australia, in 2019, where he is currently working as a Lecturer. His research interests include improving the techniques for piezoelectric energy harvesting from various vibration sources such as human motions. Recently, he developed the special harvester for human motion energy harvesting with the usage of double pendulum system.